Quasiparticle statistics and braiding from ground state entanglement

Zhang, Y.; Grover, T.; Turner, A.; Oshikawa, M.; Vishwanath, A.

DOI
10.1103/PhysRevB.85.235151
Publication date
2012
Document Version
Final published version
Published in
Physical Review B

PHYSICAL REVIEW B **85**, 235151 (2012)

Quasiparticle statistics and braiding from ground-state entanglement

Yi Zhang,[1] Tarun Grover,[1] Ari Turner,[2] Masaki Oshikawa,[3] and Ashvin Vishwanath[1,*]
[1]*Department of Physics, University of California, Berkeley, Berkeley, California 94720, USA*
[2]*University of Amsterdam, Science Park 904, P.O. Box 94485, 1090 GL Amsterdam, The Netherlands*
[3]*Institute for Solid State Physics, University of Tokyo, Kashiwa 277-8581, Japan*
(Received 27 March 2012; revised manuscript received 16 May 2012; published 29 June 2012)

Topologically ordered phases are gapped states, defined by the properties of excitations when taken around one another. Here we demonstrate a method to extract the statistics and braiding of excitations, given just the set of ground-state wave functions on a torus. This is achieved by studying the topological entanglement entropy (TEE) upon partitioning the torus into two cylinders. In this setting, general considerations dictate that the TEE generally differs from that in trivial partitions and depends on the chosen ground state. Central to our scheme is the identification of ground states with minimum entanglement entropy, which reflect the quasiparticle excitations of the topological phase. The transformation of these states allows for the determination of the modular $\mathcal{S}$ and $\mathcal{U}$ matrices which encode quasiparticle properties. We demonstrate our method by extracting the modular $\mathcal{S}$ matrix of a chiral spin liquid phase using a Monte Carlo scheme to calculate the TEE and prove that the quasiparticles obey semionic statistics. This method offers a route to nearly complete determination of the topological order in certain cases.

DOI: 10.1103/PhysRevB.85.235151 PACS number(s): 03.67.Mn, 03.65.Ud, 75.10.Kt

I. INTRODUCTION

Topologically ordered states are gapped quantum phases of matter that lie beyond the Landau symmetry breaking paradigm.[1] Well-known examples include fractional quantum Hall states and gapped quantum spin liquids.[1–10] These phases are not characterized by local correlations or order parameters but rather by long-range entanglement in their ground-state wave functions.[11] Recently, there has been renewed interest in such states, both from a fundamental perspective and with a view to applications in quantum computing.[12] At the fundamental level, topologically ordered phases display a number of unique properties. In two dimensions, emergent excitations in these states display nontrivial statistics. In Abelian topological phases, exchanging identical excitations or taking one excitation around another (braiding) leads to characteristic phase factors, which are neither bosonic nor fermionic. A further remarkable generalization of statistics occurs in non-Abelian phases where excitations introduce a degeneracy. Braiding excitations then leads to a unitary transformation on these degenerate states, which generalizes the phase factor of Abelian states.

These striking properties of topologically ordered phases are connected to excitations. An important and interesting question is whether the ground state directly encodes this information and, if so, how one may access it. It is well known that topologically ordered phases feature a ground-state degeneracy that depends on the topology of the space on which they are defined. Also, ground states of such states contain a topological contribution to the quantum entanglement, the topological entanglement entropy (TEE).[13–15] In this paper we show that, combined, these two ground-state properties can be used to extract the generalized statistics associated with excitations in these states. We apply these insights to a chiral spin liquid (CSL) wave function and numerically extract the semionic statistics associated with excitations. This demonstrates the promise of this approach for helping numerical studies diagnose the precise character of topological order in a particular state.

The generalized statistics of quasiparticles is formally captured by the modular $\mathcal{S}$ and $\mathcal{U}$ matrices, in both Abelian and non-Abelian states.[3,12,16–18] The element $\mathcal{S}_{ij}$ of the modular $\mathcal{S}$ matrix determines the mutual statistics of the ith quasiparticle with respect to the jth quasiparticle while the element $\mathcal{U}_{ii}$ of the (diagonal) $\mathcal{U}$ matrix determines the self-statistics ("topological spin") of the ith quasiparticle. Note that these provide a nearly complete description of a topologically ordered phase; for instance, fusion rules that dictate the outcome of bringing together a pair of quasiparticles are determined from the modular $\mathcal{S}$ matrix, by the Verlinde formula.[19] Previously, Wen proposed[3] using the non-Abelian Berry phase to extract statistics of quasiparticles. However, the idea in Ref. 3 requires one to have access to an *infinite set of ground states* labeled by a continuous parameter, and it is difficult to implement. Recently, Bais *et al.*[20] also discussed extracting the $\mathcal{S}$ matrix in numerical simulations, by explicit braiding of excitations. In contrast, here we just use the set of ground states on a torus to determine the braiding and fusing of gapped excitations.

Recall that the ground-state entanglement entropy of a two-dimensional topologically ordered phase in a disk-shaped region A with a smooth boundary of length L takes the form $S_A = \alpha L - \gamma$, where the universal constant γ is the TEE.[13–15] The constant γ equals $\log(D)$, where $D = \sqrt{\sum d_i^2}$ is the "total quantum dimension" associated with the topological phase, while d_i is the quantum dimension of the ith quasiparticle type. For Abelian states $d_i = 1$, so D^2 is simply the number of quasiparticle types in the theory. This is also the ground-state degeneracy on a torus. For example, the simplest case of $D^2 = 2$ corresponds to the CSL or, equivalently, the $\nu = 1/2$ bosonic Laughlin state.[21] This has, in addition to the trivial excitation, a semionic quasiparticle. Unfortunately, the total quantum dimension D only provides a partial characterization of topological order since two distinct topological phases can have the same value of D. For example, the topological phase

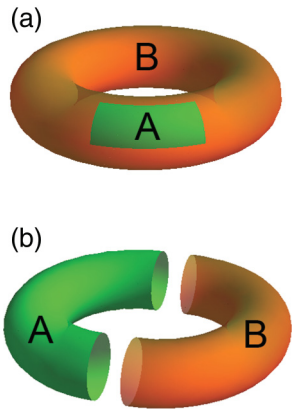

FIG. 1. (Color online) Two types of entanglement bipartitions on the torus: (a) a trivial bipartition with contractible boundaries, for which the TEE $\gamma = \log D$, and (b) a bipartition with noncontractible boundaries, where the TEE depends on the ground state.

based on a Z_2 gauge theory has $D^2 = 4$, which could also be achieved with two decoupled copies of the CSL. However, knowledge of the modular $\mathcal{S}$ matrix could tell these states apart.

It is sometimes stated without qualification that the TEE is a quantity solely determined by the total quantum dimension D of the underlying topological theory. However, this holds true *only when the boundary of region A consists of topologically trivial closed loops*. If the boundary of region A is noncontractible, for example, if one divides the torus into a pair of cylinders, *generically the entanglement entropy is different for different ground states* (see Fig. 1). Indeed, as shown in Ref. 22 for a class of topological states, the TEE depends on the particular linear combination of the ground states when the boundary of region A contains noncontractible loops. We exploit this dependence to extract information about the topological phase beyond the total quantum dimension D.

At a practical level, recent progress in numerical techniques has led to a number of proposals for topologically ordered spin-liquid phases on the Kagome,[23,24] honeycomb,[25] and square lattice with diagonal exchange.[26,27] A number of lattice states related to the Laughlin states have also been proposed in recent numerical studies.[28–32] Clearly, smoking-gun numerical signatures of topological order are increasingly needed. The procedure outlined here suggests that entanglement entropy could be used to numerically diagnose details of topological order beyond the total quantum dimension,[33–37] which is a single number susceptible to numerical error. An elegant different approach to a more complete identification of topological order is through the study of the entanglement spectrum.[38] However, we note that this requires the existence of edge states and may not be applicable for topological phases like the Z_2 spin liquid. For concreteness, consider the following problem of identifying a topological phase which is known to have quantum dimension $D = 2$. While Z_2 gauge theories have this quantum dimension, there is another theory, the doubled CSL,[39] which also has the same quantum dimension and is also time reversal symmetric. The S matrix can tell these apart, since the latter phase contains semions, and we show how the S matrix can, in principle, be extracted from the entanglement entropy. Note that the entanglement spectrum cannot tell these phases apart since they do not in general have protected edge states. Furthermore, it is possible to compute the TEE using Monte Carlo techniques on relatively larger systems,[33,37] as also done in this paper, where the entanglement spectrum is not currently available.

Let us briefly summarize the key ideas involved in this work. We recall that the number of ground states on a torus corresponds to the number of distinct quasiparticle types. Intuitively, different ground states are generated by inserting appropriate fluxes "inside" the cycle of the torus, which is only detected by loops circling the torus. We would like to express these quasiparticle states as a linear combination of ground states. A critical insight is that this can be done using the TEE for a region A that wraps around the relevant cycle of the torus. With this in hand, one can readily access the modular $\mathcal{S}$ and $\mathcal{U}$ matrices. For example, the $\mathcal{S}$ matrix is obtained by relating quasiparticle states associated with different cycles of the torus.

We begin by elaborating on the ground-state dependence of entanglement entropy, focusing on the case of a partition of torus into two cylinders (Sec. II B). We present an argument based on the strong subadditivity property of quantum information and show that the TEE per connected boundary is not identical to that for a trivial bipartition, such as a disk cut out of the torus. This is illustrated as an "uncertainty" relation, between entropies for two different cylindrical bipartitions of the torus. We introduce the notion of *minimum entropy states* (MESs), namely, the ground states with minimal entanglement entropy (or maximal TEE, since the TEE always reduces the entropy) for a given bipartition. These states can be identified with the quasiparticles of the topological phase and generated by insertion of the quasiparticles into the cycle enclosed by region A. For a generic lattice wave function with a finite correlation length, such as the CSL wave functions we study later, a nonlocal measurement like the TEE is essential to identify this basis of MESs.

In Sec. III we detail a procedure that uses the ground-state dependence of the TEE to extract the key properties of quasiparticle excitations by determining modular $\mathcal{S}$ and $\mathcal{U}$ matrices. The basic idea is to relate MESs for different entanglement bipartitions of the torus. The MESs, which reflect quasiparticle excitations, are determined using the TEE.

In Sec. IV A1 we demonstrate the ground-state dependence numerically and calculate the entanglement entropy for the CSL[21] wave function as different linear superpositions of the two ground states (Fig. 5) with the variational Monte Carlo (VMC) method.[33,40,41] This directly yields the modular $\mathcal{S}$ matrix of the CSL state, which also enables us to detect the presence of a semionic excitation in CSL. The physical origin of the ground-state dependence of the TEE is made explicit by studying a Z_2 toric code model[11] (Sec. IV B). For pedagogical purposes, in Appendix E we discuss the extraction of the modular $\mathcal{S}$ and $\mathcal{U}$ matrices for the toric code model using our algorithm.

II. GROUND-STATE DEPENDENCE OF THE TOPOLOGICAL ENTANGLEMENT ENTROPY

A. The concept of "minimum entropy states"

Given a normalized wave function $|\Phi\rangle$ and a partition of the system into subsystems A and B, one can trace out subsystem B to obtain the reduced density matrix on subsystem A: $\rho_A =$

$\mathrm{Tr}_B\,|\Phi\rangle\langle\Phi|$. The Renyi entropies are defined as

$$S_n = \frac{1}{1-n}\log\left(\mathrm{Tr}\rho_A^n\right),$$

where n is an index parameter. Taking the limit $n \to 1$, S_n recovers the definition of the usual von Neumann entropy. In this paper we often discuss the Renyi entropy with index $n = 2$, $S_2 = -\log(\mathrm{Tr}(\rho_A^2))$, since it can be calculated most easily with the VMC method[33] and, at the same time, captures all the information that we are interested in.

For a gapped phase in two dimensions with topological order and a disk -shaped region A with a smooth boundary of length L_A, the area law of the Renyi entropy gives

$$S_n = \alpha_n L_A - \gamma, \tag{1}$$

where we have omitted the subleading terms. Although the coefficient α_n of the leading "boundary law" term is nonuniversal, the subleading constant γ, which is often dubbed the TEE, is universal and a robust property of the phase of matter for which $|\Phi\rangle$ is the ground state. When region A has a disk geometry, it has been shown that the γ values for different degenerate ground states are identical and it is also insensitive to the Renyi entropy index n.[22,42] It equals $\gamma = \log D$, where D is the total quantum dimension of the model,[14,15] and offers a partial characterization of the underlying topological order.

However, when subsystem A takes a nontrivial topology, or, more precisely, when the boundary of A is noncontractible, the TEE contains more information,[22] as we elaborate further in this paper. For simplicity of illustration, throughout we focus on the case when the two-dimensional space is a torus T_2 and subsystem A wraps around the $\hat{y}$ direction of the torus and takes the geometry of a cylinder. For such a geometry, the nth Renyi entropy corresponding to the wave function $|\Phi\rangle = \sum_j c_j|\Xi_j\rangle$ is given by $S_n = \alpha_n L_A - \gamma_n'$, where $|\Xi_j\rangle$ is a special basis that we describe in detail below and γ_n' is given by[22]

$$\gamma_n'(\{p_j\}) = 2\gamma + \frac{1}{n-1}\log\left(\sum_j p_j^n d_j^{2(1-n)}\right). \tag{2}$$

Here $d_j \geqslant 1$ is the quantum dimension of the jth quasiparticle and $p_j = |c_j|^2$. For Abelian anyons, $d_j = 1$. Note that d_j shares the same subscript j as states $|\Xi_j\rangle$ because states $|\Xi_j\rangle$ can be obtained by inserting a quasiparticle with quantum dimension d_j (the ground-state degeneracy on the torus is equal to the number of distinct quasiparticles). This equation shows that the TEE for this geometry depends on the wave function through $\{p_j\}$ as well as the Renyi index n, unlike the case with disk geometry.

What is the physical significance of basis states $|\Xi_j\rangle$? We claim that these are precisely the eigenstates of the nonlocal operators defined on the entanglement cut, which distinguish the topologically degenerate ground states. For example, in the case of the quantum Hall[22] (Sec. IV A2), these states are the eigenstates of the Wilson loop operator associated with the Chern-Simons gauge field around the hole exposed by the entanglement cut. Similarly, for a Z_2 gauge theory (Sec. IV B), these are the states with definite electric and magnetic field fluxes perpendicular to the entanglement cut. For Abelian states, which have $d_j = 1$ for all j and are the focus of this paper, the entanglement entropy associated with states $|\Xi_j\rangle$ is minimum, i.e., heuristically, the entanglement cut has the maximum "knowledge" about these states. For this reason we call them MESs.

B. Strong subadditivity and topological entanglement entropy on the torus: An "uncertainty" principle

In this section we discuss the TEE for bipartitions of a torus into two cylinders. This can be done by slicing the torus in two distinct ways, along the vertical or horizontal directions. Intuitively, one might expect that both bipartitions would have the same TEE of 2γ, given the two disconnected boundaries of the cylinders. However, very general considerations based on the strong subadditivity of the von Neumann entropy alone suggest that this expectation cannot be correct. In practice, it is known that for a wide class of topological phases, the TEE of such nontrivial bipartitions indeed depends on the ground state selected.[22] Here we do not address ground-state dependence; rather we demonstrate that the TEE cannot be identical to its value for trivial bipartitions. It invokes strong subadditivity, a deep property of quantum information.[43] This will allow us to come up with an uncertainty principle, which constrains the amount of information we have when we cut the torus in two orthogonal directions. Its advantage is that it assumes almost nothing about the phase, except that it is gapped.

Consider the ground-state wave function of a gapped phase in two dimensions and three nonoverlapping subregions, A, B, and C. The von Neumann entropies S follow the strong subadditivity condition:[43]

$$S_{ABC} + S_B - S_{AB} - S_{BC} \leqslant 0. \tag{3}$$

Note that this is only known to hold for von Neumann entropies, not Renyi entropies in general. Now consider a torus with subregions A, B, and C as shown in Fig. 2. Let us decompose the entropy into a part that arises from local contributions and a nonlocal TEE, $S = S^{\mathrm{local}} + S^{\mathrm{topo}}$. For a subregion with the topology of a disk, the TEE is expected

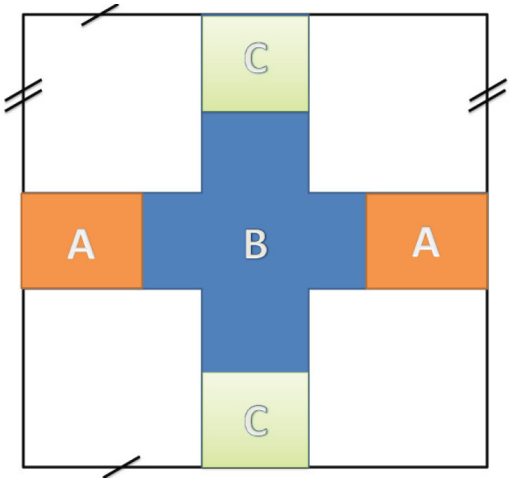

FIG. 2. (Color online) A torus, with the top, bottom, left, and right sides identified. Subregions A, B, and C are defined as shown. Regions A and C are assumed to be well separated compared to the correlation length. Regions AB and BC correspond to bipartitions of the torus into cylinders in orthogonal directions.

to be $S^{\text{topo}} = -\gamma$. Quite generally one can argue that $\gamma \geqslant 0$ utilizing the strong subadditivity condition.[14] For subregions defined on a simply connected surface, such as a disk, the TEE is proportional to the number of connected components of the boundary. If this were also true for the torus, we would expect $S^{\text{topo}}_{AB} = S^{\text{topo}}_{BC} = -2\gamma$ (since they have a a pair of boundaries). We now show that this cannot be a consistent assignment of TEE on the torus.

In order to isolate the topological part of the entropy, we assume that regions A and C are well separated compared to the correlation length of the gapped ground state. Then the local contributions cancel in the combination above: $S^{\text{local}}_{ABC} + S^{\text{local}}_{B} - S^{\text{local}}_{AB} - S^{\text{local}}_{BC} \to 0$. This can be argued following Refs. 14 and 15. For example, consider a local deformation near region A's boundary far away from the other regions. This change will be in S^{local}_{ABC}, but a nearly identical contribution will also appear in S^{local}_{AB}, since it only differs by the addition of a distant region. These will cancel in the combination above. Thus, we can rewrite Eq. (3) as

$$S^{\text{topo}}_{ABC} + S^{\text{topo}}_{B} - S^{\text{topo}}_{AB} - S^{\text{topo}}_{BC} \leqslant 0. \tag{4}$$

This inequality implies that the TEEs expected from the disk are not legal for the torus.

For regions where the boundary is topologically trivial and contractible (such as ABC or B), one expects the TEEs to be independent of the surface on which they are defined, and hence $S^{\text{topo}}_{ABC} = S^{\text{topo}}_{B} = -\gamma$. Only regions AB and BC, whose boundaries wrap around the torus, are sensitive to the topology of the space they are defined on. Their TEEs satisfy

$$\gamma_{BC} + \gamma_{AB} \leqslant 2\gamma, \tag{5}$$

where we have defined $S^{\text{topo}}_{AB(BC)} = -\gamma_{AB(BC)}$. Clearly this does not allow both the TEEs to be 2γ. In fact, if one of them attains its maximal disk value, the other must vanish. Note that the TEE reduces the total entropy. Thus, when the entropy of a cut along one of the cycles of the torus attains its minimum value, i.e., we have the most knowledge about the state on the cut, then along the orthogonal direction, the entropy associated with a cut must attain its maximal value, implying that our knowledge is the least. Therefore this can be thought of as an uncertainty relation, between cuts that wrap around different directions of the torus.

III. EXTRACTING STATISTICS FROM THE TOPOLOGICAL ENTANGLEMENT ENTROPY

The modular $\mathcal{S}$ and $\mathcal{U}$ matrices describe the action of certain modular transformations on the degenerate ground states of the topological quantum field theory. On the other hand, the braiding and statistics of quasiparticles are encoded in the $\mathcal{S}$ and $\mathcal{U}$ matrices. For Abelian phases, the ijth entry of the $\mathcal{S}$ matrix corresponds to the phase the ith quasiparticle acquires when it encircles the jth quasiparticle. The $\mathcal{U}$ matrix is diagonal and the iith entry corresponds to the phase the ith quasiparticle acquires when it is exchanged with an identical one. Since the MESs are the eigenstates of the nonlocal operators defined on the entanglement cut, the MESs are the canonical basis for defining $\mathcal{S}$ and $\mathcal{U}$. The modular matrices are just certain unitary transformations of the MES basis. As argued in Appendix D, the $\mathcal{S}$ matrix acts on MESs as an operator that implements $\pi/2$ rotation, while the $\mathcal{U}\mathcal{S}$ matrix corresponds to $2\pi/3$ rotation of MESs.

A. Algorithm for extracting the modular $\mathcal{S}$ matrix from the topoogical entanglement entropy

Since the MESs carry definite quasiparticle quantum numbers, the modular $\mathcal{S}$ matrix may be expressed as[3]

$$\mathcal{S}_{\alpha\beta} = \frac{1}{D}\langle \Xi^{\hat{x}}_{\alpha} | \Xi^{\hat{y}}_{\beta} \rangle. \tag{6}$$

Here D is the total quantum dimension and $\hat{x}$ and $\hat{y}$ are two directions on a torus. Equation (6) is just a unitary transformation between the particle states along different directions. In the case of a system with square geometry, the $\mathcal{S}$ matrix acts as a $\pi/2$ rotation on the MES basis $|\Xi^{\hat{y}}_{\beta}\rangle$. In general, however, $\hat{x}$ and $\hat{y}$ do not need to be geometrically orthogonal, and the system does not need to be rotationally symmetric, as long as the loops defining $|\Xi^{\hat{x}}_{\alpha}\rangle$ and $|\Xi^{\hat{y}}_{\beta}\rangle$ interwind with each other. Therefore, the modular $\mathcal{S}$ matrix can be derived even without any presumed symmetry of the given wave functions. Note that there is an undetermined phase for each $|\Xi^{\hat{x}}_{\alpha}\rangle$ and $|\Xi^{\hat{y}}_{\beta}\rangle$ and, therefore, a phase freedom between the rows (columns), which may be fixed by the existence of an identity particle.

Let us start with the two primitive vectors $\vec{w}_1$ and $\vec{w}_2$ that define a torus (Fig. 3) and determine the transformation of the MESs of $\vec{w}_2$ to those of $\vec{w}'_2$, given by

$$\vec{w}'_1 = n_1\vec{w}_1 + m_1\vec{w}_2, \quad \vec{w}'_2 = n_2\vec{w}_1 + m_2\vec{w}_2, \tag{7}$$

with $n_1m_2 - m_1n_2 = 1$ by definition of the modular transformation. We restrict $n_2 = -1$, which means the cross product,

$$\vec{w}_2 \times \vec{w}'_2 = -\vec{w}_2 \times \vec{w}_1 = \vec{w}_1 \times \vec{w}_2 = A. \tag{8}$$

A is the (signed) surface area of the torus.

The corresponding modular matrix can be expanded as

$$\begin{pmatrix} n_1 & 1-n_1m_2 \\ -1 & m_2 \end{pmatrix} = \begin{pmatrix} 1 & -n_1 \\ & 1 \end{pmatrix}\begin{pmatrix} & 1 \\ -1 & \end{pmatrix}\begin{pmatrix} 1 & -m_2 \\ & 1 \end{pmatrix}$$
$$= U^{-n_1}SU^{-m_2}.$$

Correspondingly, according to Appendix D the transformation

$$\mathcal{R} = \mathcal{U}^{-n_1}\mathcal{S}\mathcal{U}^{-m_2}.$$

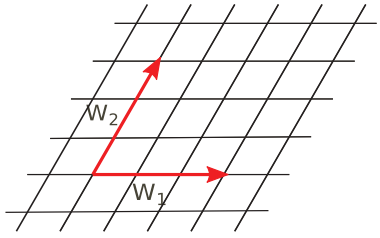

FIG. 3. (Color online) Vectors $\vec{w}_1$ and $\vec{w}_2$ define a lattice with periodic boundary conditions. That is, points differing by integer linear combinations of $\vec{w}_1$ and $\vec{w}_2$ are to be identified as the same point. The area of the lattice is $|\vec{w}_1 \times \vec{w}_2|$, where $\times$ denotes the cross product.

Because the $\mathcal{U}$ matrix is diagonal by definition, its left (right) matrix product only adds an additional phase factor to each row (column) and can be eliminated. Therefore, without any argument on the symmetry, the generalized algorithm is as follows.

(1) Given a set of ground-state wave functions $|\xi_\alpha\rangle$, calculate the TEE of an entanglement bipartition along the w_2 direction, for a linear combination $|\Phi\rangle = \sum c_\alpha |\xi_\alpha\rangle$. Search for the minimum of TEE $2\gamma - \gamma'$ in the c_α parameter space. That gives one MES $|\Xi_\beta\rangle$ and the corresponding quantum dimension $2\log(d_\beta) = 2\gamma - \gamma'$. Note that the existence of an identity particle ensures at least one minimum TEE $2\gamma - \gamma' = 0$.

(2) Iterate step 1 but with c_α in the parameter space orthogonal to all previously obtained MESs $|\Xi_\beta\rangle$. Continue this process until we have the expressions for all $|\Xi_\beta\rangle$. This gives a unitary transformation matrix U_1 with the $\alpha\beta$th entry being $c_{\alpha\beta}$, which changes the basis from $|\xi_\alpha\rangle$ to $|\Xi_\beta\rangle$. Note that there is a relative U(1) phase degree of freedom for each $|\Xi_\beta\rangle$.

(3) Repeat step 1 and step 2 but with the entanglement cut along the w_2' direction, which satisfies Eqs. (7) and (8) and obtains the unitary transformation matrix U_2.

(4) The modular $\mathcal{S}$ matrix is given by $U_2^{-1}U_1$ except for an undetermined phase for each MES corresponding to a row or a column. The existence of an identity particle that obtains a trivial phase encircling any quasiparticle helps to fix the relative phase between different MESs, requiring the entries in the first row and column to be real and positive. This completely defines the modular $\mathcal{S}$ matrix.

The above algorithm is able to extract the modular transformation matrix $\mathcal{S}$ and, hence, braiding and mutual statistics of quasiparticle excitations just using the ground-state wave functions as an input. Further, there is no loss of generality for non-Abelian phases, which can be dealt with by enforcing the orthogonality condition in step 2, which guarantees that one obtains states with quantum dimensions d_α in an increasing order.

In Appendix E we take the square lattice toric code model as an example once again, but without presuming any symmetry of the system.

B. Extracting other modular matrices from the topological entanglement entropy

In Appendix E, we calculate the $\mathcal{U}$ matrix for the Z_2 toric code model, given the simple action of $\mathcal{U}$ on $|\xi_{ab}\rangle$. Though we were unable to find a general algorithm for the $\mathcal{U}$ matrix, as we did for the the $\mathcal{S}$ matrix in Sec. III A, in the presence of certain symmetries, $\mathcal{U}$ can indeed be extracted given a set of ground-state wave functions $|\xi_\alpha\rangle$. This is achieved by first calculating the action $\mathcal{R}$ on the states $|\xi_\alpha\rangle$ under this symmetry operation and then translating it into the action on MESs. Specifically, the corresponding modular matrix is given by $U^\dagger \mathcal{R} U$, where the unitary matrix U is obtained through the first two steps of the algorithm in Sec. III A.

The aforementioned symmetry to extract the $\mathcal{S}$ matrix is the $\pi/2$ rotation, as shown in Sec. IV A3 and the first example in Appendix D, but it may be generalized to symmetries such as the rotation of other angles and even the reflection symmetry (see Appendix E). More interestingly, when the symmetry operation $\mathcal{R}$ is a $2\pi/3$ rotation, one gets the $\mathcal{US}$ matrix. Hence, if one starts with an arbitrary basis $|\xi_\alpha\rangle$ for the degenerate ground-state manifold of a topological order, the problem of $\mathcal{S}$ and $\mathcal{U}$ matrices can be reduced to the transformation property of chosen basis states $|\xi_\alpha\rangle$ under $\pi/2$ and $2\pi/3$ rotations and the unitary transformation that translates $|\xi_\alpha\rangle$ basis to the MESs $|\Xi_\alpha\rangle$. To illustrate this point, we extract the $\mathcal{US}$ matrix for the Z_2 gauge theory in Appendix E by putting the Z_2 toric code on a triangular lattice which has $2\pi/3$ rotation symmetry.

IV. DEMONSTRATION OF THE ALGORITHM TO EXTRACT STATISTICS FROM ENTANGLEMENT

A. Revisiting chiral spin liquid: Semionic statistics from entanglement entropy

In this section, to illustrate the state dependence of TEE, we study the entanglement properties in a lattice model of an SU(2) spin-symmetric CSL on a torus. The CSL has the same topological order as the half-filled Landau level $\nu = 1/2$ Laughlin state[21,44] of bosons (these bosons can be thought of as residing at the location of spin-up moments) and has twofold degenerate ground states on the torus. Even though topological properties of CSL are well established using field-theoretic methods,[3] unlike continuum Laughlin states, CSL cannot be dealt with analytically and thus provides a nontrivial demonstration of our method. In particular, the low-energy theory of CSL predicts a semion, which is difficult to verify in the lattice wave function directly. We show that our algorithm readily demonstrates the existence of a semion as an excitation in CSL, which is the main objective of this section. We note that topological order in the lattice version of CSL can be confirmed by calculating its TEE numerically using Monte Carlo and verifying that it is nonzero and agrees with the field theoretical predictions.[33] The fact that we are working with a generic lattice wave function rather than an idealized zero-correlation-length state or a topological field theory will introduce new conceptual issues; in particular, the connection between MESs and lattice ground states is discussed.

In Sec. IV A1 we demonstrate the ground-state dependence of CSL using a VMC algorithm. In Sec. IV A2, we review the basics of CSL so as to illustrate the physical meaning of CSL MESs. Finally, Sec. IV A3 illustrates our algorithm to extract the mutual statistics of quasiparticles in CSL using the entanglement data obtained using the VMC.

1. *Ground-state dependence of the topological entanglement entropy in a chiral spin liquid*

We begin by reporting the results of a numerical experiment. We extract the TEE of linear combinations of the two ground states of the CSL and show that it indeed depends systematically on the chosen linear combination, when the entanglement cut wraps around the torus. We then predict the dependence theoretically and find excellent agreement as shown in Fig. 5.

Wave functions of an SU(2) spin-symmetric CSL are obtained in the slave particle construction. We write the spins as bilinear in fermions $\vec{S} = \frac{1}{2} f_\sigma^\dagger [\vec{\sigma}]_{\sigma\sigma'} f_{\sigma'}$ and assume a chiral d-wave state for the fermions. Operationally,

the spin wave functions are obtained by Gutzwiller projection of a $d_{x^2-y^2}+id_{xy}$ superconductor to one fermion per site. More technical details regarding this wave function are given in Appendix B. We consider the system on a torus. Before projection, one can write down different fermion states by choosing the periodic or antiperiodic boundary conditions along the $\hat{x}$ and $\hat{y}$ directions. These boundary conditions are invisible to the spin degrees of freedom, which are bilinear in the fermions and lead to degenerate ground states.[4] We denote the ground states by the mean field fluxes in the $\hat{x}$ and $\hat{y}$ directions as $|\varphi_1,\varphi_2\rangle$, $\varphi_{1,2}=0,\pi$. The twofold degeneracy of the CSL implies that only two of the four ground states $|0,0\rangle$, $|\pi,0\rangle$, $|0,\pi\rangle$, and $|\pi,\pi\rangle$ are linearly independent. Here we consider linear combinations of $|0,\pi\rangle$ and $|\pi,0\rangle$, which we have numerically checked to be indeed orthogonal for the system sizes that we consider:

$$|\Phi(\phi)\rangle = \cos\phi\,|0,\pi\rangle + \sin\phi\,|\pi,0\rangle\,. \tag{9}$$

We calculated the TEE for state $|\Phi\rangle$ using the VMC method and Gutzwiller projected wave functions based on Eq. (B1). An efficient VMC algorithm which allows us to study a linear combination of Gutzwiller projected wave functions is developed and detailed in Appendix A. To our knowledge, this is the first numerical study to accomplish this.

The geometry and partition of the system are shown in Fig. 4(b). The total system size is 12 lattice spacings in both directions, with rectangles A and B being 6×4 and rectangle C 12×4. Note that subsystems AC, BC, AB, C, and ABC all wrap around the $\hat{y}$ direction so that their TEEs will all be equal (and denoted γ'). This is the quantity we wish to access. For contractible subsystems A and B it remains the same as that expected for a region with a single boundary, cut out of a topologically trivial surface (such as a bigger disk) γ. We use the construction due to Kitaev and Preskill[15] and effectively isolate the topological contributions in the limit of a small correlation length, by evaluating the combination of entropies $S_A+S_B+S_C-S_{AB}-S_{AC}-S_{BC}+S_{ABC}$. This combination is related to the TEE by

$$\begin{aligned}-2\gamma+\gamma' &= S_A+S_B+S_C-S_{AB}-S_{AC}-S_{BC}+S_{ABC}\\ &= 2S_A-2S_{AC}+S_{ABC}.\end{aligned} \tag{10}$$

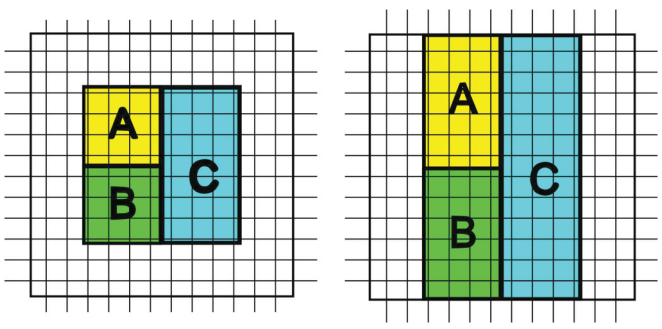

FIG. 4. (Color online) Separation of the system into subsystems A, B, and C and environment; the periodic or antiperiodic boundary condition is employed in both $\hat{x}$ and $\hat{y}$ directions. (a) Subsystem ABC is an isolated square and the measured TEE has no ground-state dependence. (b) Subsystem ABC takes a nontrivial cylindrical geometry and wraps around the $\hat{y}$ direction, and TEE may possess ground-state dependence.

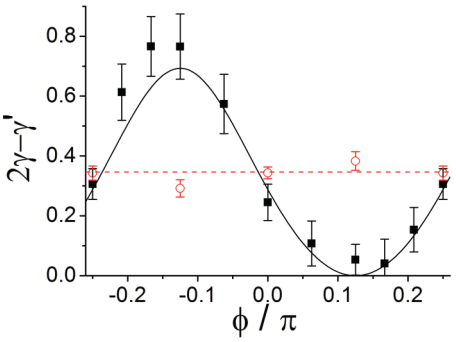

FIG. 5. (Color online) Filled (black) squares show the numerically measured TEE $2\gamma-\gamma'$ for a CSL ground state from the linear combination $|\Phi\rangle=\cos\phi\,|0,\pi\rangle+\sin\phi\,|\pi,0\rangle$ as a function of ϕ with VMC simulations using the geometry in Fig. 4(b). The solid curve is the theoretical value from Eq. (14). The periodicity is $\pi/2$. Open (red) circles show the TEE for the same linear combination for a trivial bipartition. In the latter case, the TEE is essentially independent of ϕ and, again, agrees rather well with the theoretical expectation [dashed (red) curve].

In the second line we have exploited symmetries of the construction to reduce the problem to calculation of the Renyi entropy S_2 of the three regions A, AC, and ABC for each ϕ. To measure S_2 numerically, we calculated the expectation value of a $\mathrm{Swap_A}$ operator; see Ref. 33 for an elaboration of the method used. Our results for $2\gamma-\gamma'(\phi)$ corresponding to different linear combinations parameterized by ϕ are shown in Fig. 5. This is one of the main results of this work.

We note that the TEE strongly depends on the particular linear combination chosen. The zero of the curve implies that the TEE $\gamma'=2\gamma$, the intuitive value for an entanglement cut with two boundaries. The corresponding state is the MES. We note that the MES occurs at a nontrivial angle. Understanding this requires connecting the lattice states and the field theory, which is done below. We predict this angle to be 0.125π and the overall TEE dependence to be Eq. (14), which is plotted as the solid curve in Fig. 5, in rather good agreement with the numerical data.

2. *Theoretical evaluation of the ground-state dependence of the topological entanglement entropy in chiral spin liquid wave functions*

A calculation of the ground-state dependence of the TEE involves two steps. First, we ask the following question: Given a state expressed as a linear combination of MESs, what is the expected TEE? For the CSL, this question has already been answered in Ref. 22; the TEE for a state $|\psi\rangle=a_1|1\rangle+a_2|2\rangle$ is

$$\gamma'-2\gamma=\log(|a_1|^4+|a_2|^4), \tag{11}$$

where $|1\rangle$, $|2\rangle$ are MESs for cutting the torus in the direction in question.

Second, we need to understand the relation between the MES and the physical states that appear in the Gutzwiller wave function. In general, it appears that the only way to identify MESs in a generic wave function is by calculating the TEE. However, when the lattice model has additional symmetry, which can also be used to identify MESs. Here, we have a

12×12 system defined on a square lattice and we exploit the $\pi/2$ rotation symmetry to establish a connection between the flux states $|\varphi_1, \varphi_2\rangle$ of the Gutzwiller ansatz and the MESs.

The Gutzwiller projected ground states of the CSL, $|0,0\rangle$ and $|\pi,\pi\rangle$, are clearly invariant under a $\pi/2$ rotation symmetry *up to a phase factor*. A simple calculation shows that the $|0,0\rangle$ state acquires phase factor -1, while the $|\pi,\pi\rangle$ state acquires no phase under rotation. Similarly, the states $\frac{1}{\sqrt{2}}(|0,\pi\rangle \pm |\pi,0\rangle)$ acquire a phase ± 1 under rotation. Having established the transformation of lattice states under rotation, we now study how the MESs in the field theory respond to rotations. We will see that $\pi/2$ rotation in the basis of the MESs is described by the modular $\mathcal{S}$ matrix. The eigenvectors of the modular $\mathcal{S}$ matrix will then be identified with lattice states that are rotation eigenstates.

The CSL has the same topological order as the half-filled Landau level $\nu = 1/2$ Laughlin state[21,44] of bosons. The field theory describing the topological order of a $\nu = 1/k$ Laughlin state is described by the following Chern-Simons action. Note that here only the very long wavelength degrees of freedom are retained:

$$S = \int \frac{k}{4\pi} a_\mu \partial_\upsilon a_\lambda \epsilon^{\mu\upsilon\lambda}.$$

One can define the Wilson loop operators $T_1 = e^{i\theta_1} = e^{i\oint a_x dx}$ and $T_2 = e^{i\theta_2} = e^{i\oint a_y dy}$ around the two distinct cycles of the torus. In terms of θ_i, the action is given by

$$S = i\frac{k}{2\pi}\int dt \theta_1 \dot{\theta}_2,$$

which implies that, at the operator level, $[\theta_1,\theta_2] = i\frac{2\pi}{k}$ or

$$T_1 T_2 = T_2 T_1 e^{2\pi i/k}.$$

Owing to the above relation, there are k orthogonal ground states $|\psi_m\rangle$ that can be chosen to transform under T_i as

$$T_2|\psi_m\rangle = e^{2\pi i(m-1)/k}|\psi_m\rangle, \quad T_1|\psi_m\rangle = |\psi_{m+1}\rangle.$$

In the case of a CSL phase, $k = 2$. Let us label the two degenerate ground states as $(1,0)^T$ and $(0,1)^T$, which are eigenstates of T_2:

$$T_2\,(1,0)^T = (1,0)^T, \quad T_2\,(0,1)^T = -(0,1)^T,$$
$$T_1\,(1,0)^T = (0,1)^T, \quad T_1\,(0,1)^T = (1,0)^T.$$

The last two equations are due to the commutation relation $T_1 T_2 = -T_2 T_1$. It follows that the eigenstates of T_1 are $(1,1)^T/\sqrt{2}$ and $(1,-1)^T/\sqrt{2}$.

The significance of the $T_{1,2}$ eigenstates is that they are MESs[22] for cuts whose boundaries are parallel to the loops used to define $T_{1,2}$. This is because eigenstates of these loop operators have a fixed value of flux enclosed within the relevant cycle of the torus, which minimizes the entanglement entropy for a parallel cut.

Now consider a $\pi/2$ rotation, under which $\theta_1 \to \theta_2$ and $\theta_2 \to -\theta_1$ so $T_1 \to T_2$ and $T_2 \to T_1^{-1} = T_1$. Thus, the matrix representing the effect of $\pi/2$ rotation for CSL in the T_2 eigenstate basis is

$$\mathcal{S} = \begin{pmatrix} \frac{1}{\sqrt{2}} & \frac{1}{\sqrt{2}} \\ \frac{1}{\sqrt{2}} & -\frac{1}{\sqrt{2}} \end{pmatrix}. \tag{12}$$

Note that we have used the symbol $\mathcal{S}$ for the above matrix because it is indeed the modular $\mathcal{S}$ matrix of the Chern-Simons topological quantum field theory corresponding to a CSL. We recall that the modular $\mathcal{S}$ matrix transforms the eigenstates of one Wilson loop operator T_2 to those of T_1. We return to the discussion of deriving the $\mathcal{S}$ matrix for the CSL state using the entanglement properties of the ground states in Sec. IV A3. Here we restrict ourselves to the calculation of the TEE for the CSL.

Since we are interested in the entanglement entropy with respect to a cut with noncontractible boundaries, such as the one shown in Fig. 1(b), let us represent all our states in the basis of the eigenstates of T_2, i.e., states (0,1) and (1,0). Then by matching eigenstates of the $\mathcal{S}$ matrix in the above basis and rotation eigenstates of the lattice problem, we conclude that

$$|\pi,0\rangle = \left(\sin\frac{\pi}{8}, \cos\frac{\pi}{8}\right)^T, \quad |0,\pi\rangle = \left(\cos\frac{\pi}{8}, -\sin\frac{\pi}{8}\right)^T.$$

We can now expand the general linear combination state $|\Phi(\phi)\rangle$ in MESs:

$$\begin{aligned} |\Phi\rangle &= \cos\phi\,|0,\pi\rangle + \sin\phi\,|\pi,0\rangle \\ &= \left(\cos\left(\phi - \frac{\pi}{8}\right), \sin\left(\phi - \frac{\pi}{8}\right)\right). \end{aligned} \tag{13}$$

Then, according to Eq. (2), theoretically one expects the following expression for the TEE:

$$2\gamma - \gamma' = \log\frac{4}{3 + \sin(4\phi)}, \tag{14}$$

which is compared with the numerical data in Fig. 5. The MESs occur at the value of $\phi = \pi/8 \pmod{\pi/2}$.

3. *Modular S matrix of a chiral spin liquid from the topological entanglement entropy*

Let us consider the CSL wave functions studied in Sec. IV A1 and assume that we did not have any information about the individual quantum dimensions or the modular $\mathcal{S}$ matrix. The only information that is provided is the twofold degenerate ground-state wave functions $|\pi,0\rangle$ and $|0,\pi\rangle$. We construct the linear combination $|\Phi\rangle$ as Eq. (13) and calculate its TEE for a nontrivial bipartition as Fig. 1(b) on a $\pi/2$ rotation symmetric lattice. Consequently, we get the $2\gamma - \gamma'$ dependence on parameter ϕ in Fig. 5.

We note that the minimum of the $2\gamma' - \gamma$ attained is approximately 0. According to Eq. (2), this implies that at least one of the quantum dimensions d_i should be 1. Since the total quantum dimension $D = \sqrt{d_0^2 + d_{1/2}^2} = \sqrt{2}$, this implies that $d_0 = d_{1/2} = 1$. Also, we see that the MES lies at $\phi \approx 0.14\pi$ by fitting Fig. 5 to Eq. (2).

For a system with square geometry the $\mathcal{S}$ matrix describes the action of $\pi/2$ rotation on the MESs. Since the two states $|0,\pi\rangle$ and $|\pi,0\rangle$ transform into each other under $\pi/2$ rotation, this implies that in the basis $\{|0,\pi\rangle, |\pi,0\rangle\}$, the modular $\mathcal{S}$ matrix is given by the Pauli matrix σ_x. To change the basis to MESs, we just need a unitary transformation V that rotates the $|0,\pi\rangle\,|\pi,0\rangle$ basis to the MES basis. The V is determined by the fact that one needs to rotate the $|0,\pi\rangle\,|\pi,0\rangle$ basis by an angle $\approx 0.14\pi$ to obtain the MES (this is the numerically

determined value, the exact value being $\pi/8$). Therefore,

$$\mathcal{S} = V^\dagger \begin{pmatrix} 0 & 1 \\ 1 & 0 \end{pmatrix} V,$$

where

$$V \approx \begin{pmatrix} \cos(0.14\pi) & -\sin(0.14\pi)e^{i\varphi} \\ \sin(0.14\pi) & \cos(0.14\pi)e^{i\varphi} \end{pmatrix}$$

from the two MESs—$(\cos(0.14\pi), \sin(0.14\pi))^T$ and $(-\sin(0.14\pi), \cos(0.14\pi))^T$—and φ is an undecided phase. This yields the following value for the approximate modular $\mathcal{S}$ matrix:

$$\mathcal{S} \approx \begin{pmatrix} \sin(0.28\pi) & \cos(0.28\pi)e^{i\varphi} \\ \cos(0.28\pi)e^{-i\varphi} & -\sin(0.28\pi) \end{pmatrix}.$$

The existence of an identity particle requires positive real entries in the first row and column and implies $\varphi = 0$, which gives

$$\mathcal{S} \approx \begin{pmatrix} 0.77 & 0.63 \\ 0.63 & -0.77 \end{pmatrix}.$$

Comparing this result with the exact expression in Eq. (12), we observe that even though the $\mathcal{S}$ matrix obtained using our method is approximate, some of the more important statistics can be extracted exactly. In particular, the above $\mathcal{S}$ matrix tells us that the quasiparticle corresponding to $d_0 = 1$ does not acquire any phase when it goes around any other particle and corresponds to an identity particle as expected, while the quasiparticle corresponding to $d_{1/2} = 1$ has semion statistics since it acquires a phase of π when it encircles another identical particle. Numerical improvements can further reduce the error in pinpointing the MES, thereby leading to a more accurate value of the $\mathcal{S}$ matrix. As another application, we study the action of modular transformation on the MESs $|\Xi_\alpha\rangle$ for the Z_2 gauge theory in Appendix E.

B. Toric code model: A pedagogical illustration of the algorithm

Here we use Kitaev's toric code model[11] as a pedagogical example to understand the ground-state dependence of the TEE and the nature of the MESs for a Z_2 gauge theory.

Consider the toric code Hamiltonian of spins defined on the links of a square lattice,[11]

$$H = -\sum_s A_s - \sum_p B_p, \tag{15}$$

where s and p represent the links spanned by star and plaquette as shown in Fig. 6, and $A_s = \prod_{j\in s} \sigma_j^x$, $B_p = \prod_{j\in p} \sigma_j^z$. Since all individual terms in the Hamiltonian commute with each other, ground states are constructed from the simultaneous eigenstates of all A_s and B_p. Define the operator $W^z(C)$ associated with a set of closed curves C on the bonds of the lattice, as follows:

$$W^z(C) = \prod_{j\in C} \sigma_j^z. \tag{16}$$

Then the ground state is an equal superposition of all possible loop configurations: $\sum_C W^z_{ab}(C)|\text{vac}_x\rangle$, where $|\text{vac}_x\rangle$ is a state with $\sigma_x = -1$ on every site. The closed loops are interpreted as electric field lines of the Z_2 gauge theory. We now consider two

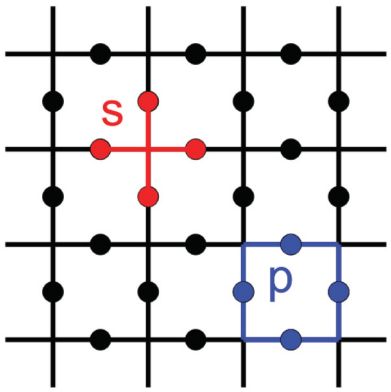

FIG. 6. (Color online) Illustration of a lattice of the toric code model; links spanned by star and plaquette are highlighted in red and blue, respectively.

geometries, first the cylinder and then the torus. The former case has a pair of degenerate ground states and is the simplest setting to demonstrate the state dependence of the TEE.

1. Cylinder geometry

On a cylinder, the Hamiltonian in Eq. (15) leads to a pair of degenerate ground states (the A_s part of the Hamiltonian is suitably modified at the boundary of the cylinder to include only three links). The two normalized ground states, $|\xi_0\rangle$ and $|\xi_1\rangle$, are given by equal superpositions of electric field loop configurations which have an even and odd winding number around the cylinder, respectively (see Fig. 7). Consider now partitioning the cylinder into two cylindrical regions, A and B. Then the Schmidt decomposition of these ground states can be written as

$$|\xi_0\rangle = \frac{1}{\sqrt{2N_q}} \sum_{\{q_l\}} \left(|\Psi^A_{\{q_l\},0}\rangle |\Psi^B_{\{q_l\},0}\rangle + |\Psi^A_{\{q_l\},1}\rangle |\Psi^B_{\{q_l\},1}\rangle \right),$$
$$|\xi_1\rangle = \frac{1}{\sqrt{2N_q}} \sum_{\{q_l\}} \left(|\Psi^A_{\{q_l\},0}\rangle |\Psi^B_{\{q_l\},1}\rangle + |\Psi^A_{\{q_l\},1}\rangle |\Psi^B_{\{q_l\},0}\rangle \right), \tag{17}$$

where the N_q distinct configurations represented by $\{q_l\}$ denote the electric field configurations at the cut. The number of field

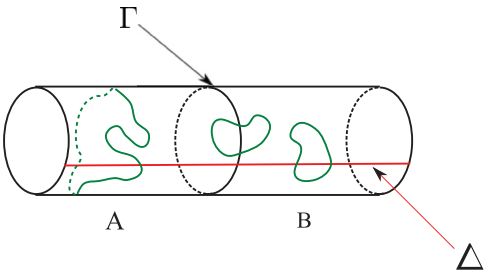

FIG. 7. (Color online) Snapshot of the ground state of the cylinder. Closed-loop strings ("Z_2 electric fields") can wrap around the cylinder. Ground states are doubly degenerate, corresponding to even- and odd-winding-number sectors. The total number of strings crossing the cut Δ equals the winding number, modulo 2. The number of strings crossing at the boundary Γ is even in the degenerate ground states.

lines crossing the cut is always even, since the ground state is composed of closed loops. For trivial bipartitions, this exhausts all terms in the Schmidt decomposition.[14] However, given that the boundary of the cut is noncontractible, the additional index 0, 1 appears, which counts the parity of the electric field winding around the cylinder, within a partition. These are correlated between the two partitions, for fixed-winding-number ground states. This is the key difference from a trivial bipartition, leading to the ground-state dependence of the TEE.

We now calculate the entanglement entropy associated with such a cut for an arbitrary linear combination of these two ground states, $|\Psi\rangle = c_0|\xi_0\rangle + c_1|\xi_1\rangle$, with unit norm. Using Eq. (17) one can easily verify that

$$|\Psi\rangle = \frac{1}{\sqrt{2N_q}} \sum_{\{q_l\}} \left[(c_0 + c_1)\left|\Psi^A_{\{q_l\},+}\right\rangle\left|\Psi^B_{\{q_l\},+}\right\rangle + (c_0 - c_1)\left|\Psi^A_{\{q_l\},-}\right\rangle\left|\Psi^B_{\{q_l\},-}\right\rangle\right], \tag{18}$$

where $|\Psi^{A(B)}_{\{q_l\},\pm}\rangle = (|\Psi^{A(B)}_{\{q_l\},0}\rangle \pm |\Psi^{A(B)}_{\{q_l\},1}\rangle)/\sqrt{2}$. For a Schmidt decomposition $|\Psi\rangle = \sum_a \sqrt{\lambda_a}|\Psi^A_a\rangle|\Psi^B_a\rangle$, the nth Renyi entropy is given by $S_n = \frac{1}{1-n}\log(\sum_a \lambda_a^n)$. We arrive at: $S_n = \frac{1}{1-n}\log N_q^{1-n}[p_+^n + p_-^n]$, where $p_\pm = |c_0 \pm c_1|^2/2$. Recognizing that the closed-loop constraint leads to $N_q = 2^{L-1}$, where L is the length of the cut, and using the definition of TEE in Eq. (1), we have

$$\gamma_n' = \log 2 - \frac{1}{1-n}\log(p_+^n + p_-^n). \tag{19}$$

Thus, for the electric field winding eigenstates $|\xi_{0,1}\rangle$, where $p_\pm = 1/2$, the TEE vanishes. However, for their equal superpositions when one of p_+ or p_- vanishes, the TEE attains its maximal value $\log 2$. These are eigenstates of the Wilson loop operator that encircles the cylinder and measures the Z_2 magnetic flux (vison number) threading it. An example of such a flux operator is $F = \prod_{j\in Q}\sigma_j^z$, where Q is a closed curve that loops once around the cylinder, such as the boundary Γ in Fig. 7. Since the TEE reduces the entanglement entropy, the maximum TEE states correspond to MESs. Why are these MESs eigenstates of flux through the cylinder for this particular cut? The number of electric field lines crossing the boundary Γ is always even. This constraint carries some information and hence lowers the entropy by bringing in the standard TEE of $\log 2$. On the other hand, the topology of the cut boundary Γ allows for a determination of which magnetic flux sector the cylinder is in. A state that is not an eigenstate of magnetic flux through the cylinder leads to a loss of information and hence a positive contribution to the total entanglement entropy (and reduces the TEE). This suggests that the MESs are eigenstates of loop operators which can be defined parallel to the cut Γ. This is further substantiated by the result for the torus case discussed below, where they are simultaneous eigenstates of magnetic flux enclosed by the cut and electric flux penetrating the cut.

2. *Torus geometry*

The four degenerate ground states are distinguished by the even-odd parity of the winding number of electric field lines around the two cycles of the torus. The operator $W^z(C)$, which generates the set of closed loops C, can be used to write the ground states:

$$|\xi_{ab}\rangle = \sum_C W^z_{ab}(C)|\mathrm{vac}_x\rangle,$$

where the subscript a (b) takes on binary values 0,1 and denotes whether the loops C belong to the even- or odd-winding-number sectors along the $\hat{x}$ ($\hat{y}$) direction, and $|\mathrm{vac}_x\rangle$ is a state with $\sigma_x = -1$ on every site. The four ground states cannot be mixed by any local operator and hence realize a Z_2 topological order. Let us consider a ground state as the following linear combination:

$$|\Psi\rangle = \sum_{a,b=0,1} c_{a,b}\,|\xi_{ab}\rangle\,. \tag{20}$$

We are interested in calculating the entanglement entropy for state $|\Psi\rangle$, corresponding to the partition shown in Fig. 1(b), and the dependence of the TEE on parameters $c_{a,b}$. After straightforward algebra (see details in Appendix C), one finds the following expression for subsystem A with boundaries of length L:

$$S_n = L\log(2) - \gamma_n'$$

where

$$\gamma_n' = 2\log(2) - \frac{1}{1-n}\log\sum_{j=1}^{4} p_j^n \tag{21}$$

and

$$p_1 = \frac{|c_{00} + c_{01}|^2}{2}, \quad p_2 = \frac{|c_{00} - c_{01}|^2}{2}, \quad p_3 = \frac{|c_{10} + c_{11}|^2}{2}, \quad p_4 = \frac{|c_{10} - c_{11}|^2}{2}. \tag{22}$$

This is indeed consistent with Eq. (2), given that $\gamma = \log D = \log 2$ and $d_j = 1$ for an Abelian topological order with $D^2 = 4$ degenerate ground states. Further, Eq. (21) readily leads to the following four MESs:

$$|\Xi_1\rangle = \frac{1}{\sqrt{2}}(|\xi_{00}\rangle + |\xi_{01}\rangle), \quad |\Xi_2\rangle = \frac{1}{\sqrt{2}}(|\xi_{00}\rangle - |\xi_{01}\rangle),$$
$$|\Xi_3\rangle = \frac{1}{\sqrt{2}}(|\xi_{10}\rangle + |\xi_{11}\rangle), \quad |\Xi_4\rangle = \frac{1}{\sqrt{2}}(|\xi_{10}\rangle - |\xi_{11}\rangle). \tag{23}$$

What is the physical significance of these four states being the MESs? Similarly to the cylinder geometry case, these states

TABLE I. Z_2 magnetic flux T_y, Z_2 electric flux F_y, and corresponding quasiparticle of the Wilson loop operator for the four MESs $|\Xi_\alpha\rangle$ of the toric code with the system geometry in Fig. 1(b). Definitions of T_y and F_y are given in Appendix C.

MES	T_y	F_y	Quasiparticle
Ξ_1	0	0	1
Ξ_2	1	0	m
Ξ_3	0	1	e
Ξ_4	1	1	em

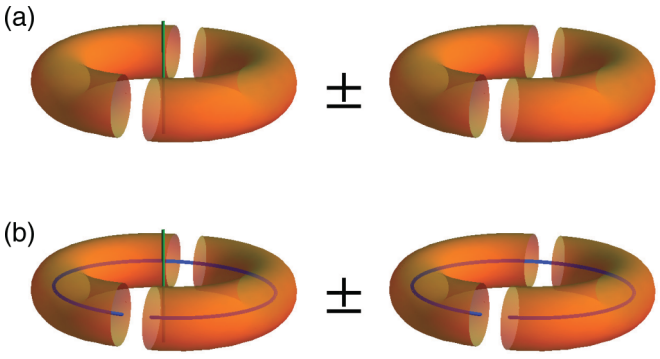

FIG. 8. (Color online) The four minimum entropy states of the Z_2 topological phase corresponding to the bipartition shown, expressed as linear combinations of the four magnetic flux states. The magnetic π flux is represented by the thick (blue and green) lines.

are the simultaneous eigenstates of the Wilson loop operator that encircles the torus and measures the Z_2 magnetic and electric fluxes threading it, as shown in Table I and Fig. 8. We leave more detailed algebra to Appendix C.

When γ_n' is maximized, the corresponding S_n is minimized, providing the maximum possible information about a given state. Since the cut is made along $\hat{y}$, it can measure the Z_2 magnetic and electric fluxes directed parallel to $\hat{x}$. Hence the MES $|\Xi_\alpha\rangle$ with definite magnetic and electric flux sectors maximizes the TEE with $\gamma_{\text{topo}} = 2\log(2)$, a contribution of $\log(2)$ from each of the two boundaries. Linear superposition of different MESs $|\Xi_\alpha\rangle$ scrambles the information obtained from magnetic and electric sectors; especially, in the extreme case of equal superposition of $|\Xi_\alpha\rangle$, all information about the global quantum numbers has been lost and we have $\gamma' = 0$. This offers another example where MESs are the eigenstates of loop operators defined on the cylinder from the entanglement cut.

V. CONCLUSION

In this paper, we have demonstrated that, on general grounds, the entanglement entropy of topologically ordered phases depends on the ground state when the entanglement cut is noncontractible. Furthermore, we have shown that this dependence can be used to extract braiding and statistics of the anyonic quasiparticles in the topological phase. We have also developed an efficient VMC algorithm to implement our algoritm to extract braiding and statistics of quasiparticles. We have illustrated the general algorithm by studying two well-known topologically ordered phases, the CSL and the Z_2 spin liquid, using the VMC method and the Z_2 toric code model analytically. We have also introduced the concept of MESs and explained their physical significance.

We note that our algorithm is completely different from the use of entanglement spectra[38] to extract universal properties of a topological phase. In particular, our algorithm is valid for all topologically ordered states, including those that do not have any edge states, such as the toric code model. In this context, we note that if edge states do exist, then the modular matrices extracted using our algorithm also determine the central charge of the edge state modulo 8.[18] Given the ground states, this algorithm determines the topological order to a large extent. We note that Wen proposed a different way to extract $\mathcal{S}$ and $\mathcal{U}$ matrices by calculating the non-Abelian Berry phase,[3] which in practice may be difficult to implement, especially on a lattice, since it requires calculating the degenerate ground states ψ_n of the system as a function of the modular parameter $\tau = \omega_2/\omega_1$ and calculating the derivatives such as $\langle\psi_n(\tau)|\partial_\tau|\psi_m(\tau)\rangle$.

We note that there may be cases where the $\pi/2$ and $2\pi/3$ rotations of the MESs may not be exactly identifiable with the modular $\mathcal{S}$ and $\mathcal{US}$ matrices, respectively. This may happen, for example, when the particles have an internal angular momentum, which may cause the wave function to acquire an additional phase upon rotation, over and above the phase due to the underlying topological structure. If the MESs correspond to spin-singlet spin-liquid wave functions (such as the CSL studied in this paper) and/or string-net models (such as the toric code model) where there is no such internal structure, there should not be such an additional phase. Further, since all MESs are locally the same, they should all acquire the same extra phase due to any local physics, and therefore, the extra phase may be separable from the topological phase.

For quantum Hall systems, because of the bulk-edge correspondence, the fusion algebra and topological spin of the bulk quasiparticles also determine the fusion rules and scaling dimensions for the primary fields in the chiral Conformal Field Theory (CFT) at the edge. Therefore, in the context of quantum Hall systems, the entanglement entropy of the ground-state manifold determines robust features of the fields in the corresponding edge CFT.

It would also be interesting to consider generalization of the methods developed in our paper to higher dimensions. Discrete gauge theories furnish the best known theories with long-range entanglement in $D \geqslant 3$ dimensions, and akin to $D = 2$, they again support degenerate ground states on the torus. It is known that these these theories again have nonzero TEE that is proportional to $\log(|G|)$, the number of elements in the gauge group.[45,46] A simple generalization of the method developed in this paper shows that the TEE for bipartition that has noncontractible boundaries will again depend on the ground state, and one will again find certain MESs that have the maximum knowledge of the quantum numbers associated with an entanglement cut. Yet as we are not aware of a simple generalization of modular transformations to higher dimensions, the meaning of the matrix that relates MESs for orthogonal entanglement cuts in higher dimensions requires further investigation.

ACKNOWLEDGMENTS

We thank Alexei Kitaev, Michael Levin, Chetan Nayak, and Shinsei Ryu for helpful discussions. A part of this research was performed at Kavli Institute for Theoretical Physics, University of California, Santa Barbara, supported by the National Science Foundation under Grant No. NSF PHY05-51164. M.O. was supported in part by Grant-in-Aid for Scientific Research (KAKENHI) No. 20102008. Y.Z., T.G., and A.V. were supported by NSF Grant No. DMR-0645691.

APPENDIX A: VARIATIONAL MONTE CARLO METHOD FOR A LINEAR COMBINATION OF WAVE FUNCTIONS

To calculate the TEE for wave functions of different linear combinations, it is important to establish a VMC algorithm for wave function as $|\Phi\rangle = \cos\phi\,|\Phi_1\rangle + \sin\phi\,|\Phi_2\rangle$, where we assume that $|\Phi_1\rangle$ and $|\Phi_2\rangle$ are properly normalized. In our case, $|\Phi_1\rangle$ and $|\Phi_2\rangle$ are two degenerate ground states, and $\langle\alpha|\Phi_1\rangle$ and $\langle\alpha|\Phi_2\rangle$ are single Slater determinants products for each configuration $|\alpha\rangle$, making $\langle\alpha|\Phi\rangle$ a sum of two Slater determinants products. However, it may also be generalized to the situation of any wave functions.

In the VMC scenario, the central quantity to evaluate in each Monte Carlo step is the ratio of $\langle\alpha'|\Phi\rangle / \langle\alpha|\Phi\rangle$, which now has the form

$$\frac{\langle\alpha'|\Phi\rangle}{\langle\alpha|\Phi\rangle} = \frac{\cos\phi\langle\alpha'|\Phi_1\rangle + \sin\phi\langle\alpha'|\Phi_2\rangle}{\cos\phi\,\langle\alpha|\Phi_1\rangle + \sin\phi\,\langle\alpha|\Phi_2\rangle}. \tag{A1}$$

It is usually much less costly to calculate the ratios $\langle\alpha'|\Phi_1\rangle/\langle\alpha|\Phi_1\rangle$ and $\langle\alpha'|\Phi_2\rangle/\langle\alpha|\Phi_2\rangle$ if $|\alpha\rangle$ and $|\alpha'\rangle$ are locally different. For our case, when $|\alpha\rangle$ and $|\alpha'\rangle$ differ by only one spin (electron) exchange, a much less costly and more accurate algorithm may be implemented for the ratio of determinants with only one different row or column. Unfortunately, after linear superimposition of different $|\Phi_i\rangle$, Eq. (A1) no longer has such a privilege.

However, one can re-express Eq. (A1) as

$$\frac{\langle\alpha'|\Phi\rangle}{\langle\alpha|\Phi\rangle} = \frac{a + bc\cdot\tan\phi}{1 + c\cdot\tan\phi},$$

where

$$a = \langle\alpha'|\Phi_1\rangle/\langle\alpha|\Phi_1\rangle, \quad b = \langle\alpha'|\Phi_2\rangle/\langle\alpha|\Phi_2\rangle$$

are again ratios of determinants and can be effectively evaluated, and

$$c = \langle\alpha|\Phi_2\rangle/\langle\alpha|\Phi_1\rangle$$

can be efficiently kept track of with $c' = a^{-1}bc$ whenever the update $|\alpha\rangle \to |\alpha'\rangle$ is accepted in a Monte Carlo step. In practice, a numerical check should be included to make sure the error for c does not accumulate too much after a certain number of Monte Carlo steps.

This algorithm may be easily generalized to the linear combination of n wave functions, with the computational cost only n times that for a single wave functions.

APPENDIX B: VARIATIONAL WAVE FUNCTION FOR A CHIRAL SPIN LIQUID

1. Chiral spin liquid from Gutzwiller projection

The lattice wave function for the CSL states that we consider are obtained using the slave-particle formalism by Gutzwiller projecting a $d + id$ BCS state.[21,44] Specifically, we Gutzwiller project the ground state of the following Hamiltonian of electrons hopping on a square lattice at half-filling:

$$H = \sum_{\langle ij\rangle} t_{ij} c_i^\dagger c_j + i\sum_{\langle\langle ik\rangle\rangle} \Delta_{ik} c_i^\dagger c_k. \tag{B1}$$

Here i and j are nearest neighbors and the hopping amplitude t_{ij} is t along the $\hat{y}$ direction and alternating between t and $-t$ in the $\hat{x}$ direction from row to row, and i and k are second nearest neighbors connected by hoppings along the square lattice diagonals, with amplitude $i\Delta_{ik} = i\Delta$ along the arrows and $i\Delta_{ik} = -i\Delta$ against the arrows (see Fig. 9). The unit cell contains two sublattices, A and B. This model leads to a gapped state at half-filling and the resulting valence band has unit Chern number. This hopping model is equivalent to a $d + id$ BCS state by an SU(2) gauge transformation. We take $\Delta = 0.5t$ to maximize the relative size of the gap and minimize the finite-size effect. Please refer to Ref. 33 for further details regarding the exact form of the wave function.

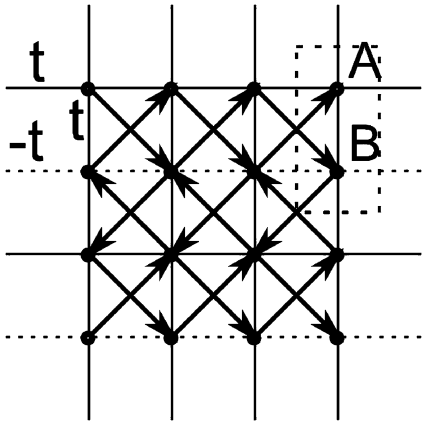

FIG. 9. Illustration of a square lattice hopping model connected with a $d + id$ superconductor. While the nearest-neighbor hopping is along the square edges with amplitude t [$(-t)$ for hopping along dashed lines], the second-nearest-neighbor hopping is along the square diagonal (bold arrows), with amplitude $+i\Delta$ $(-i\Delta)$ when the hopping direction is along (against) the arrow. The two sublattices in the unit cell are labeled A and B.

APPENDIX C: MINIMUM ENTROPY STATES OF THE TORIC CODE MODEL ON A DIVIDING TORUS

In this Appendix we Schmidt decompose the individual Toric code ground states $|\Psi\rangle$ in Eq. (20) for the bipartition of a torus in Fig. 1(b). It is helpful to introduce a virtual cut Δ which wraps around the torus in the $\hat{x}$ direction and define $|\Psi^{A(B)}_{\{q_l\},b}\rangle$ as the normalized equal superposition of all the possible configurations of closed-loop strings C in subsystem A (B) with the partition boundary condition specified by $\{q_l = 0,1\}$, $l = 1,2,\ldots,L$(so L is the total length of the boundary), and the number of crossings of the virtual cut Δ modulo 2 equals $b = 0,1$. The four ground states may now be expanded as

$$|\xi_{ab}\rangle = \frac{1}{\sqrt{2N_q}} \sum_{\{q_l\}\in a} \left(\left|\Psi^A_{\{q_l\},0}\right\rangle\left|\Psi^B_{\{q_l\},b}\right\rangle + \left|\Psi^A_{\{q_l\},1}\right\rangle\left|\Psi^B_{\{q_l\},(b+1)\bmod 2}\right\rangle\right).$$

Here $\{q_l\} \in a = 0\,(1)$ denotes that only an even (odd) number of crossings is allowed at the boundary Γ_1 (the number of crossings at the other boundary Γ_2 must be same modulo 2). $N_q = 2^{L-2}$ equals the total number of valid boundary conditions $\{q_l\} \in a$ in each parity sector.

We calculate entanglement entropy using the reduced density matrix. Here, $\rho^A = \mathrm{tr}_B|\Psi\rangle\langle\Psi|$ is readily calculated:

$$\begin{aligned}\rho^A &= \frac{1}{2N_q}\sum_{\{q_l\}\in\text{even}}\left[(|c_{00}|^2+|c_{01}|^2)\left(|\Psi^A_{\{q_l\},0}\rangle\langle\Psi^A_{\{q_l\},0}| + |\Psi^A_{\{q_l\},1}\rangle\langle\Psi^A_{\{q_l\},1}|\right) + 2\,\mathrm{Real}(c^*_{00}c_{01})\left(|\Psi^A_{\{q_l\},0}\rangle\langle\Psi^A_{\{q_l\},1}| + |\Psi^A_{\{q_l\},1}\rangle\langle\Psi^A_{\{q_l\},0}|\right)\right]\\ &+ \frac{1}{2N_q}\sum_{\{q_l\}\in\text{odd}}\left[(|c_{10}|^2+|c_{11}|^2)\left(|\Psi^A_{\{q_l\},0}\rangle\langle\Psi^A_{\{q_l\},0}| + |\Psi^A_{\{q_l\},1}\rangle\langle\Psi^A_{\{q_l\},1}|\right) + 2\,\mathrm{Real}(c^*_{10}c_{11})\left(|\Psi^A_{\{q_l\},0}\rangle\langle\Psi^A_{\{q_l\},1}| + |\Psi^A_{\{q_l\},1}\rangle\langle\Psi^A_{\{q_l\},0}|\right)\right]\\ &= \frac{1}{2N_q}\sum_{\{q_l\}\in\text{even}}\left[|c_{00}+c_{01}|^2|\Psi^A_{\{q_l\},+}\rangle\langle\Psi^A_{\{q_l\},+}| + |c_{00}-c_{01}|^2|\Psi^A_{\{q_l\},-}\rangle\langle\Psi^A_{\{q_l\},-}|\right] + \frac{1}{2N_q}\sum_{\{q_l\}\in\text{odd}}\left[|c_{10}+c_{11}|^2|\Psi^A_{\{q_l\},+}\rangle\langle\Psi^A_{\{q_l\},+}|\right.\\ &\left.+|c_{10}-c_{11}|^2|\Psi^A_{\{q_l\},-}\rangle\langle\Psi^A_{\{q_l\},-}|\right].\end{aligned}$$

Here $|\Psi^A_{\{q_l\},\pm}\rangle = \frac{1}{\sqrt{2}}(|\Psi^A_{\{q_l\},0}\rangle \pm \Psi^A_{\{q_l\},1}\rangle)$ and the orthogonality conditions holds.

From the above expression, it immediately follows that the Renyi entanglement entropy S_n is given by Eq. (21):

$$\begin{aligned}S_n &= \frac{1}{1-n}\log\left(\mathrm{Tr}\rho_{\mathrm{A}}^{\mathrm{n}}\right)\\ &= \frac{1}{1-n}\log\left(\left(\frac{1}{2N_q}\right)^n\cdot N_q\left(\sum_{j=1}^{4}(2p_j)^n\right)\right)\\ &= \log N_q + \frac{1}{1-n}\log\sum_{j=1}^{4}p_j^n\\ &= L\log 2 - \left(2\log 2 + \frac{1}{n-1}\log\sum_{j=1}^{4}p_j^n\right),\end{aligned}$$

where p_j are defined in Eq. (22).

To understand the nature of the corresponding MES in Eq. (23), we first discuss the quasiparticle excitations of the toric code model. Imagine defining the following string operator on the links of the lattice

$$W^z(O) = \prod_{j\in O}\sigma_j^z.$$

Now $W^z(O)|\mathrm{vac}_x\rangle$ is an excited state and still an eigenstate of A_s and B_p, with $A_s = -1$ at the two ends of O. We may regard them as electric charge quasiparticles that cost a finite energy to create and the string connecting them as an electric field line. To return to the ground state, the electric charges need to be annihilated by each other. One way to do this is to wrap the open string O parallel to $\hat{x}$ around the cycle of the torus. O becomes a closed loop C, yet this changes the parity of the electric field winding number along $\hat{x}$. We define the electric charge loop operator that inserts an additional electric field in the $\hat{x}(\hat{y})$ direction by the above procedure as a Z_2 electric flux insertion operator $T_x(T_y)$.

$$\begin{aligned}T_x|\xi_{1b}\rangle &= |\xi_{0b}\rangle, \quad T_x|\xi_{0b}\rangle = |\xi_{1b}\rangle,\\ T_y|\xi_{a1}\rangle &= |\xi_{a0}\rangle, \quad T_y|\xi_{a0}\rangle = |\xi_{a1}\rangle.\end{aligned} \tag{C1}$$

There is also a magnetic field, which determines the phase of the electric charge as it moves. In particular, when there is a magnetic field along the $\hat{y}$ direction of the torus of 1(0) total flux (mod 2), the electric charge picks up a minus (plus) sign traveling around the loop in the $\hat{x}$ direction, and similarly for the magnetic field along the $\hat{x}$ direction. Denoting the insertion operator of such Z_2 magnetic flux as F_y and F_x, the loop operators of the magnetic charge (vison), we have

$$T_xF_y = -F_yT_x, \quad T_yF_x = -F_xT_y.$$

They suggest that $T_x(T_y)$ is the magnetic flux measuring operator in the $\hat{y}(\hat{x})$ direction and $F_x(F_y)$ is the electric flux measuring operator in the $\hat{y}(\hat{x})$ direction. Note that both the electric and the magnetic flux are defined modulo 2 in correspondence with the Z_2 gauge theory. After simple algebra,

$$F_y|\xi_{ab}\rangle = (-1)^a|\xi_{ab}\rangle, \quad F_x|\xi_{ab}\rangle = (-1)^b|\xi_{ab}\rangle. \tag{C2}$$

Comparing Eqs. (C1) and (C2) with Eq. (23), we arrive at the conclusions listed in Table I.

APPENDIX D: MODULAR TRANSFORMATIONS

The $\mathcal{S}$ and $\mathcal{U}$ matrices describe the action of modular transformations on the degenerate ground states of the topological quantum field theory on a torus. For Abelian phases, the ijth entry of the $\mathcal{S}$ matrix corresponds to the phase the ith quasiparticle acquires when it encircles the jth quasiparticle. The $\mathcal{U}$ matrix is diagonal and the iith entry corresponds to the phase the ith quasiparticle acquires when it is exchanged with an identical one. Let us first review the geometric meaning of these transformations. Labeling our system by complex coordinates $z = x + iy$, the torus may be defined by the periodicity of ω_1 and ω_2 along the two directions $\hat{e_1}$ and $\hat{e_2}$ (which need not be orthogonal), i.e., $z \equiv z + \omega_1 \equiv z + \omega_2$. Now consider a transformation

$$\begin{pmatrix}\omega_1\\ \omega_2\end{pmatrix} \to \begin{pmatrix}\omega_1'\\ \omega_2'\end{pmatrix} = \begin{pmatrix}a & b\\ c & d\end{pmatrix}\begin{pmatrix}\omega_1\\ \omega_2\end{pmatrix}, \tag{D1}$$

where $a,b,c,d \in \mathbb{Z}$. Since our system lives on a lattice, the inverse of the above matrix should again have integer components, hence the determinant $ad - bc = 1$. One can show that matrices with these properties form a group, called $SL(2,\mathbb{Z})$. Interestingly, all the elements in this group can be obtained by a successive application of the following two generators of $SL(2,\mathbb{Z})$:

(1) $S = \left(\begin{smallmatrix}0 & 1\\ -1 & 0\end{smallmatrix}\right)$. This transformation corresponds to $\omega_1 \to \omega_2$ and $\omega_2 \to -\omega_1$ and therefore, for a square geometry, corresponds to rotation of the system by 90^o.

(2) $U = \left(\begin{smallmatrix}1 & 1\\ 0 & 1\end{smallmatrix}\right)$. Under this transformation $\omega_1 \to \omega_1' = \omega_1 + \omega_2$ and $\omega_2 \to \omega_2' = \omega_2$. Consider a loop on the torus with

winding numbers n_1 and n_2 along the ω_1 and ω_2 directions. By definition of the U transformation, the winding numbers in the transformed basis,

$$\begin{aligned} n_1\omega_1 + n_2\omega_2 &= n_1(\omega_1' - \omega_2') + n_2\omega_2' \\ &= n_1'\omega_1' + n_2'\omega_2', \end{aligned}$$

where $n_1' = n_1$ and $n_2' = n_2 - n_1$ are the winding numbers along the ω_1' and ω_2' directions.

The transformation properties of the resulting MESs under modular transformations would yield the desired $\mathcal{S}$ and $\mathcal{U}$ matrices. Further, for a symmetry transformation of $F(S,U)$ on $(\omega_1,\omega_2)^T$, the corresponding modular transformation on MESs would yield the modular $\mathcal{F}(\mathcal{S},\mathcal{U})$ matrix.

In the main text, we have obtained $\mathcal{S}$ and $\mathcal{U}$ matrices for the toric code model from the action of these transformations on the basis states $|\xi_{ab}\rangle$. We now show that one can also obtain the $\mathcal{US}$ matrix by studying the action of $2\pi/3$ rotation $R_{2\pi/3}$ on the MESs (provided that $R_{2\pi/3}$ is the symmetry of the model). To see this, consider a triangular lattice that is defined by two lattice vectors (complex numbers) ω_1 and ω_2, with $\omega_1 = (1,0)$ and $\omega_2 = (1/2,\sqrt{3}/2)$. The transformation of our interest is the transformation of ω_1,ω_2 under $R_{2\pi/3}$ rotation: $\omega_1 \to \omega_1' = -\omega_1 + \omega_2$ and $\omega_2 \to \omega_2' = -\omega_1$. Therefore, one can write the $R_{2\pi/3}$ matrix:

$$R_{2\pi/3} = \begin{pmatrix} -1 & 1 \\ -1 & 0 \end{pmatrix}. \tag{D2}$$

This matrix belongs to the group $SL(2,\mathbb{Z})$ and simple algebra shows that $R_{2\pi/3} = US$. One may also check that $R_{2\pi/3}^3 = 1$, as one might expect. Therefore, knowing the action of $R_{2\pi/3}$ on the MESs would lead to the $\mathcal{US}$ matrix.

APPENDIX E: MODULAR MATRICES OF Z_2 GAUGE THEORY BY TRANSFORMING MINIMUM ENTROPY STATES

Let us study the action of modular transformation on the MESs $|\Xi_\alpha\rangle$ for the Z_2 gauge theory in Sec. IV B and compare the resulting modular matrices with the known results. First, consider a $\pi/2$ rotation symmetric square sample. Under $\pi/2$ rotation, $|\xi_{ab}\rangle \to |\xi_{ba}\rangle$. According to Eq. (23), the transformations for the MESs $|\Xi_\alpha\rangle$ for cuts along $\hat{y}$ are

$$\begin{aligned} |\Xi_1\rangle &\to \tfrac{1}{2}\left(|\Xi_1\rangle + |\Xi_2\rangle + |\Xi_3\rangle + |\Xi_4\rangle\right), \\ |\Xi_2\rangle &\to \tfrac{1}{2}\left(|\Xi_1\rangle + |\Xi_2\rangle - |\Xi_3\rangle - |\Xi_4\rangle\right), \\ |\Xi_3\rangle &\to \tfrac{1}{2}\left(|\Xi_1\rangle - |\Xi_2\rangle + |\Xi_3\rangle - |\Xi_4\rangle\right), \\ |\Xi_4\rangle &\to \tfrac{1}{2}\left(|\Xi_1\rangle - |\Xi_2\rangle - |\Xi_3\rangle + |\Xi_4\rangle\right). \end{aligned}$$

Hence, the modular $\mathcal{S}$ matrix is given by

$$\mathcal{S} = \frac{1}{2}\begin{pmatrix} 1 & 1 & 1 & 1 \\ 1 & 1 & -1 & -1 \\ 1 & -1 & 1 & -1 \\ 1 & -1 & -1 & 1 \end{pmatrix}.$$

This is exactly what one expects from the topological quantum field theory corresponding to the zero-correlation-length deconfined-confined Z_2 gauge theory. There are four flavors of quasiparticles in the spectrum—1, m, e, and em—as we have reported in Table I. The electric charge e and magnetic charge (vison) m both have self-statistics of a boson and pick up a phase of π when they encircle each other (and, as a corollary, the same phase when they encircle em). By studying $\mathcal{S}$, one gets the self and mutual statistics for quasiparticles encircling each other.

In Sec. III A we further show that symmetry is not required to determine the $\mathcal{S}$ matrix. In Eq. (23) we have shown the MESs for cuts along the $w_2 = \hat{y}$ direction:

$$\begin{aligned} |\Xi_1\rangle &= \frac{e^{i\varphi_1}}{\sqrt{2}}(|\xi_{00}\rangle + |\xi_{01}\rangle), \quad |\Xi_2\rangle = \frac{e^{i\varphi_2}}{\sqrt{2}}(|\xi_{00}\rangle - |\xi_{01}\rangle), \\ |\Xi_3\rangle &= \frac{e^{i\varphi_3}}{\sqrt{2}}(|\xi_{10}\rangle + |\xi_{11}\rangle), \quad |\Xi_4\rangle = \frac{e^{i\varphi_4}}{\sqrt{2}}(|\xi_{10}\rangle - |\xi_{11}\rangle), \end{aligned}$$

where φ_i are undetermined phases for MESs $|\Xi_i\rangle$. The unitary matrix U_1 connecting the w_2 MESs and the electric flux states,

$$U_1 = \frac{1}{\sqrt{2}}\begin{pmatrix} e^{i\varphi_1} & e^{i\varphi_2} & & \\ e^{i\varphi_1} & -e^{i\varphi_2} & & \\ & & e^{i\varphi_3} & e^{i\varphi_4} \\ & & e^{i\varphi_3} & -e^{i\varphi_4} \end{pmatrix}. \tag{E1}$$

On the other hand, it is straightforward to verify that for loops along the $w_2' = -\hat{x} + \hat{y}$ direction, which satisfies our requirement, Eq. (8), the corresponding MESs

$$\begin{aligned} |\Xi_1'\rangle &= \frac{e^{i\varphi_1'}}{\sqrt{2}}(|\xi_{00}\rangle + |\xi_{11}\rangle), \quad |\Xi_2'\rangle = \frac{e^{i\varphi_2'}}{\sqrt{2}}(|\xi_{00}\rangle - |\xi_{11}\rangle), \\ |\Xi_3'\rangle &= \frac{e^{i\varphi_3'}}{\sqrt{2}}(|\xi_{01}\rangle + |\xi_{10}\rangle), \quad |\Xi_4'\rangle = \frac{e^{i\varphi_4'}}{\sqrt{2}}(|\xi_{01}\rangle - |\xi_{10}\rangle); \end{aligned}$$

again, φ_i' are undetermined phases for MESs $|\Xi_i'\rangle$. The unitary matrix U_2 connecting the w_2' MESs and the electric flux states

$$U_2 = \frac{1}{\sqrt{2}}\begin{pmatrix} e^{i\varphi_1'} & e^{i\varphi_2'} & & \\ & & e^{i\varphi_3'} & e^{i\varphi_4'} \\ & & e^{i\varphi_3'} & -e^{i\varphi_4'} \\ e^{i\varphi_1'} & -e^{i\varphi_2'} & & \end{pmatrix}. \tag{E2}$$

Combining Eqs. (E1) and (E2), we can write down the modular $\mathcal{S}$ matrix as

$$\begin{aligned} \mathcal{S} &= U_2^{-1}U_1 \\ &= \frac{1}{2}\begin{pmatrix} e^{i(\varphi_1-\varphi_1')} & e^{i(\varphi_2-\varphi_1')} & e^{i(\varphi_3-\varphi_1')} & -e^{i(\varphi_4-\varphi_1')} \\ e^{i(\varphi_1-\varphi_2')} & e^{i(\varphi_2-\varphi_2')} & -e^{i(\varphi_3-\varphi_2')} & e^{i(\varphi_4-\varphi_2')} \\ e^{i(\varphi_1-\varphi_3')} & -e^{i(\varphi_2-\varphi_3')} & e^{i(\varphi_3-\varphi_3')} & e^{i(\varphi_4-\varphi_3')} \\ e^{i(\varphi_1-\varphi_4')} & -e^{i(\varphi_2-\varphi_4')} & -e^{i(\varphi_3-\varphi_4')} & -e^{i(\varphi_4-\varphi_4')} \end{pmatrix}. \end{aligned}$$

To ensure the existence of an identity particle in accord with the first row and column, we impose the conditions

$$\varphi_1' = \varphi_2' = \varphi_3' = \varphi_4' = \varphi_1 = \varphi_2 = \varphi_3 = \varphi_4 + \pi.$$

This leads to the following modular $\mathcal{S}$ matrix:

$$\mathcal{S} = \frac{1}{2}\begin{pmatrix} 1 & 1 & 1 & 1 \\ 1 & 1 & -1 & -1 \\ 1 & -1 & 1 & -1 \\ 1 & -1 & -1 & 1 \end{pmatrix},$$

which is indeed the correct result for the Z_2 toric code.

Now consider the transformation corresponding to the $\mathcal{U}$ matrix as described in Appendix D, where $n_1' = n_1$ and

$n_2' = n_2 - n_1$ are the winding numbers along the ω_1' and ω_2' directions. Using this expression and Eq. (23), the transformation for MESs from w_2 cut to w_2' cut,

$$|\Xi_1\rangle \to |\Xi_1\rangle, \quad |\Xi_2\rangle \to |\Xi_2\rangle,$$
$$|\Xi_3\rangle \to |\Xi_3\rangle, \quad |\Xi_4\rangle \to -|\Xi_4\rangle.$$

This leads to the following modular $\mathcal{U}$ matrix:

$$\mathcal{U} = \begin{pmatrix} 1 & 0 & 0 & 0 \\ 0 & 1 & 0 & 0 \\ 0 & 0 & 1 & 0 \\ 0 & 0 & 0 & -1 \end{pmatrix}.$$

Again, this is what is expected from the Z_2 gauge theory. The sign of -1 on the last entry of the diagonal corresponds to the fermionic self-statistics of the em, while the positive signs correspond to the bosonic self-statistics of 1, e, and m particles.

To see a more generic example of deriving the $\mathcal{U}$ matrix from rotation symmetry, we first define the toric code on a triangular lattice, with system dimensions such that the $2\pi/3$ rotation is a symmetry of the system. The Hamiltonian is the same as Eq. (15), with the star $''s''$ denoting six links emanating from a vertex, while the plaquette $''p''$ now involves three links. We again denote the four degenerate ground states on a torus as $|\xi_{ab}\rangle$, with $a,b = 0,1$ denoting the parity of the electric field along the noncontractible cycles. The relation between MESs $|\Xi_\alpha\rangle$ and states $|\xi_{ab}\rangle$ remains unchanged [Eq. (23)]. The calculation for the transformation under $2\pi/3$ proceeds analogously to that for $\pi/2$ rotation and one finds

$$R_{2\pi/3}|\xi_{00}\rangle = |\xi_{00}\rangle, \quad R_{2\pi/3}|\xi_{01}\rangle = |\xi_{10}\rangle,$$
$$R_{2\pi/3}|\xi_{10}\rangle = |\xi_{11}\rangle, \quad R_{2\pi/3}|\xi_{11}\rangle = |\xi_{01}\rangle.$$

Translating the action of $R_{2\pi/3}$ on states $|\xi_\alpha\rangle$ to that on states $|\Xi_\alpha\rangle$, one finds

$$\mathcal{US} = \frac{1}{2}\begin{pmatrix} 1 & 1 & 1 & 1 \\ 1 & 1 & -1 & -1 \\ 1 & -1 & 1 & -1 \\ -1 & 1 & 1 & -1 \end{pmatrix}.$$

Combining the expression and the $\mathcal{S}$ matrix, one obtains

$$\mathcal{U} = \begin{pmatrix} 1 & 0 & 0 & 0 \\ 0 & 1 & 0 & 0 \\ 0 & 0 & 1 & 0 \\ 0 & 0 & 0 & -1 \end{pmatrix}$$

as expected.

*Corresponding author: ashvinv@socrates.berkeley.edu

[1] X.-G. Wen, *Quantum Field Theory of Many-Body Systems: From The Origin of Sound to an Origin of Light and Electrons* (Oxford Graduate Texts, Oxford University Press, New York, 2004).
[2] P. W. Anderson, Science **237**, 1196 (1987).
[3] X.-G. Wen, Int. J. Mod. Phys. B **4**, 239 (1990).
[4] N. Read and B. Chakraborty, Phys. Rev. B **40**, 7133 (1989).
[5] X.-G. Wen, Phys. Rev. B **44**, 2664 (1991).
[6] N. Read and S. Sachdev, Phys. Rev. Lett. **66**, 1773 (1991); S. Sachdev, Phys. Rev. B **45**, 12377 (1992).
[7] T. Senthil and M. P. A. Fisher, Phys. Rev. B **62**, 7850 (2000).
[8] R. Moessner and S. L. Sondhi, Phys. Rev. Lett. **86**, 1881 (2001).
[9] P. A. Lee, Rep. Prog. Phys. **71**, 012501 (2008).
[10] L. Balents, Nature **464**, 199 (2010).
[11] A. Kitaev, Ann. Phys. **303**, 2 (2003).
[12] See, e.g., C. Nayak, S. H. Simon, A. Stern, M. Freedman, and S. D. Sarma, Rev. Mod. Phys. **80**, 1083 (2008).
[13] A. Hamma, R. Ionicioiu, and P. Zanardi, Phys. Lett. A **337**, 22 (2005); Phys. Rev. A **71**, 022315 (2005).
[14] M. Levin and X.-G. Wen, Phys. Rev. Lett. **96**, 110405 (2006).
[15] A. Kitaev and J. Preskill, Phys. Rev. Lett. **96**, 110404 (2006).
[16] E. Keski-Vakkuri and X.-G. Wen, Int. J. Mod. Phys. B **7**, 4227 (1993).
[17] P. Di Francesco, P. Mathieu, and D. Senechal, *Conformal Field Theory* (Springer, New York, 1997).
[18] A. Kitaev, Ann. Phys. **321**, 2 (2006).
[19] E. P. Verlinde, Nucl. Phys. B **300**, 360 (1988).
[20] F. A. Bais and J. C. Romers, arXiv:1108.0683v1.
[21] V. Kalmeyer and R. B. Laughlin, Phys. Rev. Lett. **59**, 2095 (1987); Phys. Rev. B **39**, 11879 (1989); X. G. Wen, Frank Wilczek, and A. Zee, *ibid*. **39**, 11413 (1989).
[22] S. Dong, E. Fradkin, R. G. Leigh, and S. Nowling, J. High Energy Phys. 05 (2008) 016.
[23] S. Yan, D. A. Huse, and S. R. White, Science **332**, 1173 (2011).
[24] H.-C. Jiang, Z. Y. Weng, and D. N. Sheng, Phys. Rev. Lett. **101**, 117203 (2008).
[25] Z. Y. Meng, T. C. Lang, S. Wessel, F. F. Assaad, and A. Muramatsu, Nature **464**, 847 (2010).
[26] H.-C. Jiang, H. Yao, and L. Balents, arXiv:1112.2241.
[27] L. Wang, Z.-C. Gu, F. Verstraete, and X.-G. Wen, arXiv:1112.3331.
[28] D. N. Sheng, Z. C. Gu, K. Sun, and L. Sheng, Nature Commun. **2**, 389 (2011).
[29] E. Tang, J. W. Mei, and X. G. Wen, Phys. Rev. Lett. **106**, 236802 (2011).
[30] T. Neupert, L. Santos, C. Chamon, and C. Mudry, Phys. Rev. Lett. **106**, 236804 (2011).
[31] Y.-F. Wang, H. Yao, Z.-C. Gu, C.-D. Gong, and D. N. Sheng, Phys. Rev. Lett. **108**, 126805 (2012).
[32] N. Regnault and B. A. Bernevig, Phys. Rev. X **1**, 021014 (2011).
[33] Y. Zhang, T. Grover, and A. Vishwanath, Phys. Rev. Lett. **107**, 067202 (2011); Phys. Rev. B **84**, 075128 (2011).
[34] S. Furukawa and G. Misguich, Phys. Rev. B **75**, 214407 (2007).
[35] M. Haque, O. Zozulya, and K. Schoutens, Phys. Rev. Lett. **98**, 060401 (2007); O. S. Zozulya, M. Haque, K. Schoutens, and E. H. Rezayi, Phys. Rev. B **76**, 125310 (2007).
[36] H. Yao and X.-L. Qi, Phys. Rev. Lett. **105**, 080501 (2010).
[37] S. V. Isakov, M. B. Hastings, and R. G. Melko, Nature Phys. **7**, 772 (2011).
[38] H. Li and F. D. M. Haldane, Phys. Rev. Lett. **101**, 010504 (2008).
[39] M. A. Levin and X.-G. Wen, Phys. Rev. B **71**, 045110 (2005).
[40] C. Gros, Ann. Phys. **189**, 53 (1989).
[41] M. B. Hastings, I. Gonzalez, A. B. Kallin, and R. G. Melko, Phys. Rev. Lett. **104**, 157201 (2010).

[42]S. T. Flammia, A. Hamma, T. L. Hughes, and X. G. Wen, Phys. Rev. Lett. **103**, 261601 (2009).

[43]M. A. Nielsen and I. L. Chuang, *Quantum Computation and Quantum Information* (Cambridge University Press, Cambridge, 2000).

[44]D. F. Schroeter, E. Kapit, R. Thomale, and M. Greiter, Phys. Rev. Lett. **99**, 097202 (2007).

[45]C. Castelnovo and C. Chamon, Phys. Rev. B **78**, 155120 (2008).

[46]Y. Zhang, T. Grover, and A. Vishwanath, Phys. Rev. B **84**, 075128 (2011).